[CANCER RESEARCH 64, 6010–6017, September 1, 2004]

Tumor-dependent Kinetics of Partial Pressure of Oxygen Fluctuations during Air and Oxygen Breathing

L. Isabel Cárdenas-Navia,[1] Daohai Yu,[2] Rod D. Braun,[3] David M. Brizel,[1] Timothy W. Secomb,[4] and Mark W. Dewhirst[1]

Departments of [1]Radiation Oncology and [2]Biostatistics and Bioinformatics, Duke University Medical Center, Durham, North Carolina; [3]Department of Anatomy/Cell Biology, Karmanos Cancer Institute, Wayne State University School of Medicine, Detroit, Michigan; and [4]Department of Physiology, Arizona Health Sciences Center University of Arizona, Tucson, Arizona

ABSTRACT

The primary purpose of this study was to examine the kinetics of partial pressure of oxygen (pO_2) fluctuations in fibrosarcoma (FSA) and 9L tumors under air and O_2 breathing conditions. The overall hypothesis was that key factors relating to oxygen tension fluctuations would vary between the two tumor types and as a function of the oxygen content of the breathing gas. To assist in the interpretation of the temporal data, spatial pO_2 distributions were measured in 10 FSA and 8 9L tumors transplanted into the subcutis of the hind leg of Nembutal-anesthetized (50 mg/kg) Fischer 344 rats. Recessed-tip oxygen microelectrodes were inserted into the tumor, and linear pO_2 measurements were recorded in 50-μm steps along a 3-mm path, and blood pressure was simultaneously measured via femoral arterial access. Additionally, pO_2 was measured at a single location for 90 to 120 minutes in FSA ($n = 11$) or 9L tumors ($n = 12$). Rats were switched from air to 100% O_2 breathing after 45 minutes. Temporal pO_2 records were evaluated for their potential radiobiological significance by assessing the number of times they crossed a 10-mm-Hg threshold. In addition, the data were subjected to Fourier analysis for air and O_2 breathing.

FSA and 9L tumors had spatial median pO_2 measurements of 4 and 1 mm Hg, respectively. 9L had more low pO_2 measurements ≤2.5 mm Hg than did FSA, whereas between 2.5 and 10 mm Hg this pattern was reversed. Pimonidazole staining patterns in FSA and 9L tumors supported these results. Temporal pO_2 instability was observed in all experiments during air and O_2 breathing. Threshold analyses indicated that the 10 mm Hg threshold was crossed 2 to 5 times per hour, independent of tumor type. However, the magnitude of 9L pO_2 fluctuations was approximately eight times greater than FSA fluctuations, as assessed with Fourier transform analysis (Wilcoxon, $P < 0.005$). O_2 breathing significantly increased median pO_2 in FSA from 3 to 8 mm Hg ($P < 0.005$) and caused a significant increase in frequency and magnitude of pO_2 fluctuations. One hundred percent O_2 breathing had no effect on 9L tumor pO_2, and it decreased the magnitude of pO_2 fluctuations with borderline significance.

These results show that these two tumors differ significantly with respect to spatial and temporal oxygenation conditions under air and O_2 breathing. Fluctuations of pO_2 of the type reported herein are predicted to significantly affect radiotherapy response and could be a source for genetic instability, increased angiogenesis, and metastases.

INTRODUCTION

Tumor hypoxia is classically depicted as developing as a result of two independent phenomena: chronic hypoxia caused by limitations of oxygen diffusion, and transient hypoxia caused by microvessel flow instabilities.

Although intermittent blood flow and hypoxia have been studied extensively with indirect methods, such as dye mismatch (1, 2), laser Doppler flowmetry (3), and hypoxia markers (4, 5), direct measurement of partial pressure of oxygen (pO_2) instability has been done only on the R3230Ac tumor with recessed tip microelectrodes (6, 7) and on two human tumor xenograft lines with a fiber optic oxygen sensor (8, 9). It is important to determine the characteristics of intermittent hypoxia in other tumor types with direct methods. Direct measurements of kinetics provide unique information about the frequency of subregions existing under radiobiologically significant pO_2 conditions. In addition, the magnitude of fluctuations can be determined. Both of these variables may be important in governing treatment response and in altering gene expression patterns that could indirectly influence tumor cellular behavior.

The main focus of this article is on the temporal instability in pO_2 during air and O_2 breathing. Spatial pO_2 distributions were also performed for these two tumors to facilitate interpretation of the transient data. Oxygen tension distributions of two tumor lines that grow in the Fischer 344 rat, a fibrosarcoma (FSA; ref. 10) and 9L glioma (9L; ref. 11), were performed, using methods identical to those used previously for the R3230Ac tumor. Second, the kinetics of pO_2 fluctuation were examined under air- and oxygen-breathing conditions.

MATERIALS AND METHODS

Animal Model

Forty-one female Fischer 344 rats (Charles River Laboratories, Raleigh, NC) were used in this study. Twenty-one rats received subcutaneous implants of 1- to 2-mm^3 pieces of a rat fibrosarcoma in the left hind limb. The remaining twenty received cell injections of four to six million 9L glioma cells grown in Eagle's basal medium supplemented with 10% fetal calf serum and 5% fibrinogen (cells obtained courtesy of K. Wheeler, Wake Forest University, Winston Salem, NC). After the tumors had reached 1 to 1.5 cm in diameter, rats were anesthetized with an intraperitoneal injection of 50 mg/kg pentobarbital sodium. The femoral artery and vein were cannulated for recording of blood pressure and venous access, respectively. A small portion (~4–10 mm^2) of the skin and tumor capsule was removed to expose the tumor surface for microelectrode insertion. The surface was moistened by topical application of saline. A small incision was made in the left forelimb and a Ag/AgCl reference electrode was sutured into the subcutis. Body temperature was maintained at 37°C by placing the rat on a regulated water-heated blanket (K-module, Baxter Healthcare, Valencia, CA).

Oxygen Microelectrodes

Recessed-tip microelectrodes were produced using a previously published technique (12, 13). The electrodes had tip diameters of 8.9 (6.1–12.7) μm (13 electrodes) and recess lengths of ~30 μm. Microelectrodes were polarized at −0.7 V using a commercial polarizing box and a picoammeter unit (Chemical microsensor no. 1201, Diamond General, Ann Arbor, MI). Electrodes were calibrated before and after experiments in a 37°C saline-filled tonometer alternately bubbled with 0, 2.5, 5 or 15% O_2 (balance nitrogen). An *in vivo* zero value was obtained by recording microelectrode current in tissue after euthanasia of the rat with an overdose of pentobarbital sodium. The average sensitivity of the electrodes was 0.93 (0.73–1.5) mm Hg picoampere.

Received 4/9/03; revised 5/13/04; accepted 7/9/04.

Grant support: Supported by a grant from the NIH/Nation Cancer Institute CA40355.

The costs of publication of this article were defrayed in part by the payment of page charges. This article must therefore be hereby marked *advertisement* in accordance with 18 U.S.C. Section 1734 solely to indicate this fact.

Requests for reprints: Mark Dewhirst, Box 3455, Room 201 MSRB, Research Drive, Duke University Medical Center, Durham, NC 27710. Phone: 919-684-4180; Fax: 919-684-8718; E-mail: dewhirst@radonc.duke.edu.

Spatial Profiles of Tumor Partial Pressure of Oxygen

These measurements were done using methods reported previously (14). Briefly, a micromanipulator (model MO102E, Narishige, Narishige, Japan) was positioned so that a dummy electrode could reach the exposed tumor surface, covered in a drop of saline. The actual electrode was then placed in the micromanipulator and advanced into the saline droplet. It was allowed to polarize and then was advanced into the tumor. Total measurement length for each track was 3 mm (50 μm/step) with 3 to 4 tracks per tumor (mean of 198 measurements per tumor). After experiments were completed, rats were sacrificed using Euthasol (Delmarva Laboratories, Midlothian, VA), and the *in vivo* zero value for the microelectrode was recorded. Cumulative frequency distributions were obtained for each animal and then were averaged over each tumor type to obtain means and 95% exact confidence intervals for specific pO_2 intervals in the histogram. Partial pressure of oxygen distributions were measured in 18 rats (10 FSA and 8 9L).

Histology and Immunohistochemistry

Pimonidazole. Five rats, three FSA and two 9L, were given injections of 70 mg/kg pimonidazole before spatial profiles of pO_2 were completed. Three hours after injection and after the pO_2 profiles had been completed, the animals were sacrificed. The tumor was removed from the rat and was fixed in 70% formalin before being paraffin embedded within 24 to 48 h. Immunohistochemistry for pimonidazole (hypoxia marker) was carried out as described previously (15).

Temporal Variations in Blood Flow and Tumor Partial Pressure of Oxygen

Anesthetized rats were placed on a temperature-controlled water-heated blanket, and the left leg was stabilized on a rubber pedestal with tape. The arterial cannula was connected to a blood pressure transducer and amplifier (model 11-G4143-01, Gould Instruments, Valley View, OH), and the amplifier signal was digitized at 25 Hz and recorded using data acquisition software (AT-CODAS, Windaq, DATAQ Instruments, Akron, OH). Two laser Doppler-flow probes (outer diameter, 480 μm) were inserted into the tumor on the side opposite from the exposed surface. The probes were connected to the flowmeter and data acquisition system (Oxford Array, Oxford Optronix, Oxford, United Kingdom), which acquires data at 20 Hz.

An oxygen microelectrode was inserted into the tumor, using the same method as described above. The microelectrode was moved several millimeters into the tissue until a clearly non-zero pO_2 value was obtained, allowing the possibility for the pO_2 to increase or decrease. The electrode then remained fixed for the rest of the study. Rats breathed air for 45 minutes and were then switched to 100% O_2 for an additional 45 minutes. During the full 90 minutes, pO_2, blood pressure, and laser Doppler blood flow were continuously recorded. Twenty-three rats were used for this study (11 FSA and 12 9L).

Fourier Analysis

Fourier analyses of temporal variation in blood flow and pO_2 were performed using commercial software included in the data acquisition package (CODAS, DATAQ Instruments, Akron, OH). Blood pressure and pO_2 recordings could be analyzed directly within the program, because the same software was used to acquire the data. The blood flow data were transferred from the Oxford array system to ASCII text files, which were then converted to CODAS files.

The frequency characteristics of the instrumentation had no impact on the Fourier analysis. The oxygen microelectrodes respond within 40 to 400 milliseconds (13), which is much faster than the fluctuations of interest in this study. Although the high-frequency response of the Chemical Microsensor no. 1201 is somewhat limited in the range (200 picoamperes full scale) that was used in most cases, its cutoff (3 decibels) frequency was 2.3 Hz (138 cycles/min). According to the manufacturer, the Oxford laser Doppler array has a cutoff frequency of 5 Hz (300 cycles/min). Because these cutoff frequencies are relatively high, the resulting attenuation had little or no effect on the apparent power within the frequency range of interest. Therefore, the instrumentation did not contribute to nor did it bias the pO_2 or laser Doppler flowmetry signals.

One record length was analyzed using the Fourier analysis: 33 minutes for pO_2 and blood pressure; 34 minutes for blood flow. The analysis was performed on records that contained 49,146 points (blood pressure and pO_2) or 40,960 points (blood flow). The software averaged the records over every 5 or 6 points to obtain files 8,192 points in length. For the recordings during air breathing, each record overlapped the previous record by 50%. For example, the first Fourier analysis of a pO_2 recording covered data from 0.0 to 32.8 minutes, the second from 12.0 to 44.9 minutes. The Fourier analysis of pO_2 during O_2 breathing was performed on the data recorded between 57.0 and 89.8 minutes.

Analysis of Power Spectra

Frequency. An informative way to view and compare frequency information from Fourier power spectra is to examine the frequencies at which the power peaks (7, 16).

Power and Magnitude of Fluctuations. The power of the Fourier power spectra (*i.e.*, the magnitude of the fluctuations) was analyzed by examining the total power over a given frequency range (17). Because most of the power in the present study was at very low frequencies, the range chosen for this analysis was 0 to 10 cycles/min. The total power of a spectrum was obtained by a summation of all powers between 0 cycles/min and a given frequency.

Statistical Analysis

Partial Pressure of Oxygen Distribution Analysis. The relative and cumulative frequencies of the spatial pO_2 data were plotted against the pO_2 and analyzed using SAS (SAS Institute, Cary, NC). The point estimate and its exact confidence interval were computed for each type of tumor for both relative and cumulative frequencies (averaged across tracks first, and then across experimental units for each type of tumor). Parametric (*t* test) as well as nonparametric (Wilcoxon and Normal score) tests were carried out for informal comparisons between the two tumor types at each histogram interval. A smoothing version of the histogram technique was explored using SAS procedure kernel density estimation to estimate the density and distribution of the data. The mixed effects model was also used to examine relative or cumulative frequency with respect to tumor type, using a random intercept to account for multiple pO_2 measurements from multiple tracks of one tumor. The results from the last two approaches, however, were very similar to those from the histogram methods and, therefore, are not discussed in detail.

Fourier Analysis of pO_2 and Blood Flow Fluctuations. The cumulative magnitude or power in millimeters of $(\text{mercury})^2$ $[(\text{mm Hg})^2]$ of pO_2 fluctuations and its 95% confidence interval were first found on the log scale to make its distribution more normal-like and avoid getting a negative lower confidence limit. Data were then transformed back to the original scale. The cumulative power of pO_2 was compared between tumor types for air and O_2 breathing, using the Wilcoxon rank test performed at each frequency point of interest. The difference between O_2 and air was compared within each tumor type using the signed rank test as well as between tumor types using Wilcoxon and normal score tests.

Changes in pO_2 of Radiobiological Significance during Air and O_2 Breathing. For hypoxia-reoxygenation kinetics, Wilcoxon and Van der Wearden normal score or χ^2 (for categorical variables) tests were used to assess for differences between tumor types in total duration and number of episodes, and median pO_2 during hypoxic episodes or the entire interval. A signed rank test was used to assess differences between O_2 and air breathing within each tumor type, and the difference between O_2 and air breathing across the two tumor types was assessed, as before, using Wilcoxon and Van der Wearden normal score tests.

Unless otherwise stated, all of the values presented in the text are medians with interquartile ranges (IQRs).

RESULTS

Spatial Partial Pressure of Oxygen Distributions

The median pO_2 values were 4 (2–8) mm Hg and 1 (0–7) mm Hg for FSA and 9L tumors, respectively. By comparison, the median value for the R3230Ac has been reported to be 4 mm Hg (14). FSA and 9L both have ~80% of their pO_2 values below 10 mm Hg, but between 0 and 10 mm Hg, there are differences between the tumor

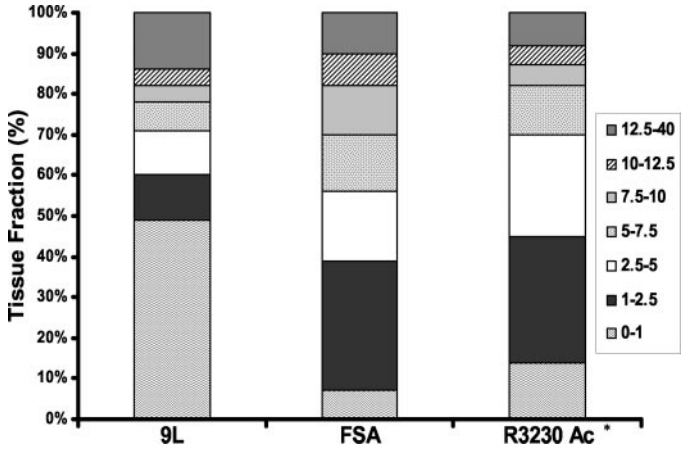

Fig. 1. FSA, 9L, and R3230Ac tumor lines all have 80 to 90% of the tissue fraction below 10 mm Hg; however, 9L has a much larger fraction of its tissue at values less than or equal to 1 mm Hg, and FSA and R3230Ac both have larger fractions (~50%) of moderately hypoxic regions between 1 and 5 mm Hg. See Table 1 for statistical comparisons. *, from previously published data (1).

Table 1 *Summary of partial pressure of oxygen histogram data*

pO_2 range (in mm Hg)	Fraction of values*	
	9L	FSA
<1.0	49 (29–58)†	7 (2–13)†
<2.5	60 (48–71)†	39 (31–48)†
<5.0	71 (58–79)†	56 (46–64)†
<7.5	78 (66–84)	70 (58–77)†
<10.0	82 (70–87)	82 (72–87)
<12.5	86 (74–90)	90 (81–93)
<40.0	100 (94–100)	100 (94–100)

* Percentages shown as means (95% confidence intervals).
† Significantly different from other tumor type.

types (Fig. 1; Table 1). 9L has a greater proportion of severely hypoxic pO_2 values (<2.5 mm Hg) than does FSA, which has the majority of its hypoxic values in an intermediate range (5–7.5 mm Hg). 9L had a significantly higher (71 *versus* 56%) cumulative percentage of pO_2 values ≤ 5 mm Hg compared with FSA ($P < 0.05$).

Histology and Immunohistochemistry

Pimonidazole. Examples from two tumors are shown in Fig. 2. FSA shows well-oxygenated regions near the edge of the tumor, but also has large regions of moderate hypoxia, shown as light brown staining throughout the tumor. The central region of the tumor also shows small patches of dark brown staining, indicating regions of severe hypoxia. Small regions of necrosis also appear along the bottom edge of the figure. 9L pimonidazole staining shows several dark brown patches indicating severe hypoxia very close to well-oxygenated regions. This tumor also shows many regions of necrosis, surrounded by regions of moderate to severe hypoxia.

Intermittent Hypoxia

The time interval of the pO_2 measurements averaged 97.2 (92.3–104.0) minutes for FSA, and 93.3 (92.0–95.1) minutes for 9L. The median heart rate for all animals was 345 (321–371) beats per minute (bpm) for the minute previous to beginning O_2 breathing, and 342 (324–370) bpm for the last 33 minutes of O_2 breathing. Mean arterial blood pressure averaged 111 (104–116) and 116 (112–120) mm Hg for air and O_2 breathing, respectively. Thus, systemic cardiovascular conditions were stable during these experiments and within the range reported for unanesthetized rats (18).

Air *versus* Oxygen Breathing Results

Tumor pO_2 Fluctuations. Tumor pO_2 fluctuations were measured in 11 FSA, and 12 9L tumors. An example of one FSA tumor recording is shown in Fig. 3*A*. In this example, pO_2 remained fairly constant during the air-breathing period, staying between 4–5 mm Hg. After O_2 breathing was started, pO_2 gradually increased to nearly 15 mm Hg. The magnitude of fluctuations changed with the switch from air to O_2. During air breathing, fluctuations varied less than ~1 mm Hg. After the rat began breathing O_2, the magnitude of fluctuations increased to 4 to 5 mm Hg (Fig. 3*A*). For FSA overall, the median pO_2 value during the 30 minutes before O_2 breathing was 3 (2–12) mm Hg, and it rose to 8 (4–25) mm Hg during the 30-minute period beginning 12 minutes after the onset of O_2 breathing. The increase in pO_2 was statistically significant ($P < 0.005$, signed rank test).

Fig. 3*B* shows one trace of a 9L tumor pO_2 recording. During the first 48 minutes of air breathing, pO_2 fluctuated and then gradually dropped from 16 to 2 mm Hg. The magnitude of fluctuations of pO_2 visibly decreased when the rat was switched to O_2 breathing (Fig. 3*B*). The median of pO_2 values during the last 30 minutes of air breathing was 9 (6–18) mm Hg, and was 9 (1–15) mm Hg before O_2 breathing. Thus, pO_2 did not significantly change in this tumor type on switching from air to O_2 breathing ($P = 0.34$).

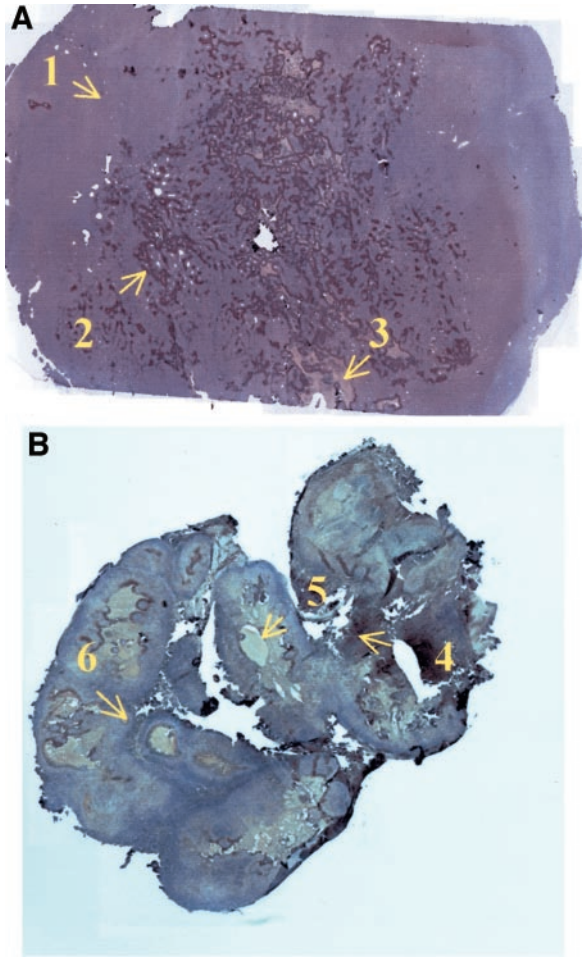

Fig. 2. Examples of pimonidazole staining in FSA (*A*) and 9L (*B*). FSA shows large regions of moderate hypoxia (*arrow 1*) and regions of well-oxygenated tissue. There are also small patches of severe hypoxia (*arrow 2*), and some necrosis (*arrow 3*). 9L pimonidazole staining shows large patches of severe hypoxia (*arrow 4*) and necrosis (*arrow 5*). There are also regions of severe hypoxia very close to well-oxygenated regions (*arrow 6*).

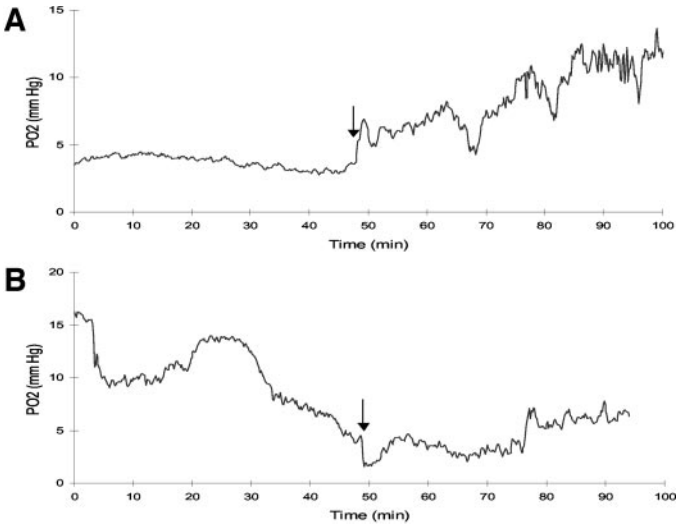

Fig. 3. Examples of temporal pO_2 traces for FSA (*A*) and 9L (*B*); *arrow*, the time at which the rat was switched from air to oxygen breathing. For FSA, pO_2 increased with the onset of O_2 breathing. The 9L tumor trace shows an immediate slight decrease in pO_2 when O_2 breathing began, but the level then returned to the baseline pO_2 a few minutes later.

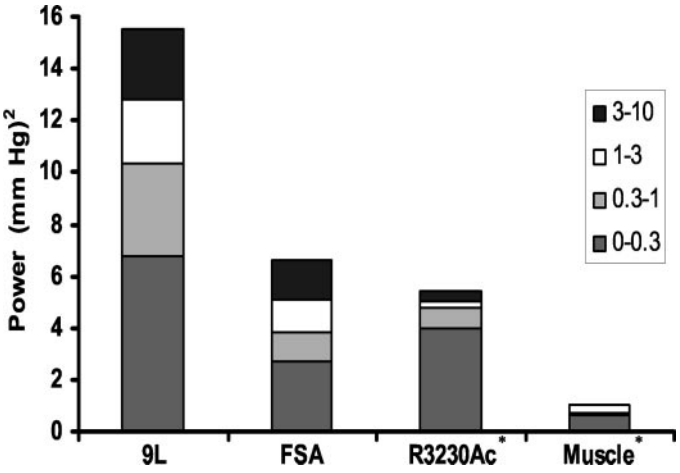

Fig. 4. Summary of pO_2 power *versus* fluctuation frequency for tumor lines and normal muscle. 9L has greater cumulative power than FSA, R3230Ac, and muscle tissue over all frequencies shown. FSA and 9L have a large portion of their cumulative power occurring at higher frequencies (0.3–10 cpm), whereas most of the cumulative power for R3230Ac occurs between 0 and 0.3 cpm. FSA cumulative power is roughly equivalent to that of the R3230Ac, both of which were higher in cumulative power than muscle tissue over all frequencies shown. *, from previously published data (9).

Changes in pO_2 of Radiobiological Significance during Air and O_2 Breathing. FSA and 9L pO_2 traces during air and O_2 breathing were examined with respect to a 10-mm Hg threshold value for hypoxia. A threshold of 10 mm Hg was chosen because, below this value, radiosensitivity is most sensitive to changes in pO_2. Any two hypoxic episodes separated by less than 30 seconds were collapsed into a single episode, under the condition that the difference in the median pO_2 between the two episodes was not greater than 5 mm Hg. After combining those episodes, if the duration of a hypoxic episode was no more than 10 seconds, it was treated as a nonhypoxic episode. These rules were set, keeping in mind that a typical radiation fraction usually requires several minutes to apply. Thus, very short periods of hypoxia would not likely affect radioresponse appreciably. Experiments for each tumor were classified as not showing hypoxia-reoxygenation if they remained either above or below the 10-mm-Hg threshold for the 30-minute observation during air breathing and the 30-minute observation during O_2 breathing (Table 2). For both tumor types, the number of times per hour that pO_2 crossed the 10-mm-Hg threshold ranged from 0 to 10 was an average of 2. The frequency of threshold crossing was independent of the breathing gas.

For FSA the change from air to O_2 breathing caused tumor pO_2 to increase. During O_2 breathing, fewer tumors always remained below 10 mm Hg, down from seven tumors during air to four during O_2 breathing. Of those FSA tumors that fluctuated below the al threshold, the pO_2 of the hypoxic intervals significantly increased during O_2 breathing ($P < 0.05$, signed rank test).

For the 9L tumor, there was no significant difference ($P = 0.34$) in pO_2 comparing air (median, 9 mm Hg) to O_2 breathing (median, 9 mm Hg). The median pO_2 during hypoxic episodes, however, decreased with borderline significance from 6 mm Hg during air breathing to 1 mm Hg during O_2 breathing ($P = 0.08$, signed rank test), which was opposite to the change in median FSA pO_2.

Fourier Analysis of Tumor pO_2 Fluctuations. Fourier analysis showed that pO_2 fluctuations typically occurred at very low frequencies (<1 cpm) for both FSA and 9L tumors. There were differences in the power spectra however (Fig. 4). The cumulative power of 9L is greater than FSA, indicating that fluctuations in 9L pO_2 were signif-

Table 2 *Summary of partial pressure of oxygen fluctuations across a 10 mm Hg threshold*

	FSA		9L	
Variable	Air $pO_2 < 10$	O_2 $pO_2 < 10$	Air $pO_2 < 10$	O_2 $pO_2 < 10$
Never hypoxic*	3 of 11	4 of 11	3 of 12	3 of 12
Always hypoxic	7 of 11	4 of 11	3 of 12	3 of 12
No. available for fluctuation analysis	8 of 11	7 of 11	9† of 12	9‡,§ of 12
Median no. of events/h (range) for all tumors	2 (0–2)	2 (0–6)	2 (0–8)	2 (0–10)
Median % time (range) hypoxic	100 (0–100)	77 (0–100)	62 (0–100)	79 (0–100)
Median no. of minutes (range) hypoxic	30 (0–30)	23 (0–30)	19 (0–30)	24 (0–30)
Median pO_2 (range) during interval‖	3 (1–15)¶,**,††	8 (0–31)¶,††	9 (1–22)**,††	9 (0–32)††
Median pO_2 (range) during hypoxic episodes‡‡	2 (0–8)§§,‖‖,††	5 (0–9)‖‖,††	6 (1–10)§§,††	1 (0–9)††

* Hypoxic is defined as $pO_2 < 10$ mm Hg for at least 20 seconds (pO_2 was averaged over 10-second intervals).
† One tumor with a hypoxic duration of 29 minutes and 10 seconds out of 30 minutes.
‡ One tumor with a hypoxic duration of 29 minutes and 50 seconds out of 30 minutes.
§ One tumor with a median hypoxic pO_2 of 0 for a hypoxic duration of 28 minutes and 20 seconds out of 30 minutes.
‖ Median pO_2 during the interval is the median pO_2 of the entire set of tumors for the full 30-minute period of analysis.
¶ $P < 0.005$ signed rank for air *versus* O_2.
** $P < 0.05$ Wilcoxon for FSA *versus* 9L.
†† $P < 0.006$ Wilcoxon for FSA *versus* 9L in the difference between air and O_2.
‡‡ Median pO_2 during hypoxic episodes is the median pO_2 below the 10-mm-Hg threshold for the subset of tumors available for fluctuation analysis.
§§ $P < 0.05$ Wilcoxon for FSA *versus* 9L.
‖‖ $P < 0.05$ signed rank for air *versus* O_2.

icantly larger than in FSA ($P < 0.005$, Wilcoxon). The power spectra are similar between FSA and previously published data for R3230Ac (7). The power spectra for all tumors are greater than that which has been reported for normal rat muscle, using identical measurement methods (7).

Tumor Blood Flow Fluctuations. Tumor blood flow was measured at two sites in seven rats with FSA and nine rats with 9L tumors. Small variations of ~5% in blood flow occurred continuously in all of the tumors. In general, however, the range of fluctuations for blood flow was less then 30%, with 9L showing greater changes in relative blood flow than did FSA. Temporal characteristics of the two recordings made at different sites in the same tumor varied, with some tumors showing two completely independent traces and some tumors showing two temporally coordinated traces. There was no discernable change in fluctuations of relative blood flow for either FSA or 9L when the animal was switched from air to O_2.

Fourier Analysis of Tumor Blood Flow Fluctuations. Fourier analysis showed dominant fluctuations occurring at low frequencies (<1 cpm) for FSA and 9L tumors, although contributing frequencies occurred over the range of 0 to 10 cpm (data not shown). There were differences in the power spectra, showing that the cumulative power of the 9L was greater than that of FSA during air breathing, particularly at low frequencies, although they did not reach statistical significance. O_2 breathing did not affect the frequency distribution appreciably for either tumor.

Fourier Analysis of Changes in Frequency and Power in pO_2 and Blood Flow after Switch from Air to O_2 Breathing. There was a significant increase in frequency of O_2 fluctuations in FSA during O_2 breathing between 0 and 10 cpm (data not shown). There was also a borderline significant increase in magnitude of fluctuations over the frequency range (0–10 cpm), with mean increases on the order of 400%. The relative frequency of fluctuations for 9L tumors was not changed when going from air to O_2 (data not shown). In contrast to FSA, however, there was a borderline significant decrease in the fluctuation magnitude (power) over the 0 to 10 cpm frequency range. The change in power spectra when switching from air to O_2 breathing between FSA and 9L in the fluctuation power was statistically significant ($P = 0.01$, Wilcoxon). FSA and 9L blood flow showed no significant changes in frequency or power with the switch from air to O_2 breathing.

DISCUSSION

Spatial Partial Pressure of Oxygen Distributions

These tumor lines were similar as assessed by pO_2 histograms, yet they were quite different with respect to details of the distribution. For comparison, previously published data for R3230Ac are included (7). Fig. 1 shows that all three tumors had a similar percentage of tissue below 10 mm Hg, that is, between 80 and 90%. However, 9L has a much larger fraction of its tissue at values less than or equal to 1 mm Hg, and FSA and R3230Ac both have a larger fraction of moderately hypoxic tissue (between 1 and 5 mm Hg) than does 9L. These measurements are in qualitative agreement with the pimonidazole staining seen in Fig. 2.

The 9L glioma showed large track lengths of pO_2 near zero, alternating with track lengths that were well above 10 mm Hg. This tumor is typically reported to have a very small radiobiological hypoxic fraction (11), but some investigators have found it to be radiobiologically hypoxic (19). In these experiments, we suspect that the long track lengths of near-zero pO_2 corresponded to zones of necrosis. The discontinuity, between the electrode histograms and what is known about the radiobiological hypoxic fraction, points to one of the primary difficulties of using electrode measurements to predict radiation response. If measurements are made in areas of necrosis or nonclonogenic cells, the resultant electrode hypoxic fraction will overestimate the radiobiological hypoxic fraction (20, 21). The radiation response of FSA has not yet been determined, although the data from this study suggest that O_2 breathing would probably improve the radiation response.

Partial Pressure of Oxygen Fluctuations

Temporal Changes in pO_2 and Radiobiological Significance. Description of temporal instability in tumor oxygenation can be done several ways based on measurements from this report. Important features of the description should include (*a*) the percentage of time that pO_2 lies within a radiobiologically significant range and the frequency that this occurs within a given experiment, and (*b*) the percentage of measurements in which pO_2 fluctuates into the range that would be considered radiobiologically important. These features of the temporal instability could influence radiotherapy response (3). The magnitude of the changes in pO_2 is also important, because this may influence the susceptibility of the tissue to hypoxia-reoxygenation injury.

We did not perform any experiments in which we observed stable pO_2 values. Stability here is defined as remaining at a value within the resolution limit of the electrodes, which is 1 mm Hg. This does not mean that all tumor regions are in a state of unstable oxygenation, however. Because we required a non-zero baseline pO_2 (to allow for increases or decreases in pO_2 over time), we selected for better oxygenated areas that might be more susceptible to fluctuations in pO_2 than areas of lower overall baseline pO_2. For example, the average pO_2 from the histogram measurements in the 9L tumor was 1 mm Hg, whereas the average pO_2 for the fluctuant oxygenation measurements was 14 ± 9 mm Hg. In contrast, the same pO_2 values averaged 4 and 8 ± 2 mm Hg for FSA, respectively. There was no significant difference in baseline pO_2 measurements between the two tumor lines for the fluctuation studies ($P = 0.11$). This minimizes the chance that there was selection bias that could have influenced the analysis of hypoxia fluctuation results.

Approximately 30% of the experiments remained above a 10-mm-Hg threshold for the duration of the kinetic study and, therefore, were not in a radiobiologically significant range. Similarly, some experiments remained below this threshold for the duration of the study (Table 2). For those experiments in which the threshold was crossed, the average number of crossings per hour was 2, regardless of the tumor type or the breathing gas. These results were similar to those published previously for the R3230Ac tumor (6, 7).

In recently published articles (22), we used the experimentally derived data from the present work to model the effects of pO_2 instabilities on radiotherapy response. For conventionally fractionated radiotherapy, we predicted that tumor control probability would be dominated by the average pO_2 observed during the 30-minute interval of observation. For more coarse fractionation schemes, such as stereotactic radiosurgery (six-field technique) or intraoperative radiotherapy with a high-dose-rate remote after-loading method, tumor control probability was substantially reduced, compared with conventional external beam fractionation, because there is increased likelihood that at least some of the treatment time is dominated by low pO_2 conditions. Oxygen enhancement ratio did not average near the maximal value of 3 in any experiments, indicating that the pO_2 fluctuations simulate a moderate degree of hypoxia and, therefore, a moderate degree of radioresistance. Wouters and Brown (23) have argued that cells of intermediate radiosensitivity are likely to dominate radiotherapy response, based on the argument that full reoxygenation does not

occur between fractions of radiation. Our data support the conclusion that intermediate levels of hypoxia are dominant, but this comes from a completely different logic, based on the direct measurements of pO_2 transients.

Kinetics of pO_2 Fluctuations. There is a substantial body of evidence supporting the idea that temporal kinetics of pO_2 and blood flow fluctuation in other rodent models and in human tumors are dominated by relatively slow fluctuations, on the order of 2 to 5 cycles per hour. For example, the radiation response of cells located near and far from perfused vessels, as marked with the perfusion marker drug Hoechst 33342, has been examined when the dye was given before or simultaneously with radiotherapy (3). When animals received the dye and were irradiated simultaneously, brightly stained cells were clearly more radiosensitive, supporting the theory that cells located nearer to vessels would be better oxygenated. However, when several minutes expired (typically 20–30 min) between dye administration and irradiation, the radiosensitivity of brightly and dimly stained cells was the same. These data suggested that, in the intervening minutes between dye administration and irradiation, some cells that were aerobic became hypoxic and *vice versa*. The 20-to-30-minute time interval to see this effect is consistent with our observation of cycle times on the order of 2 to 5 events per hour.

Similar conclusions have been made using pairs of fluorescent dyes that could be given either simultaneously or separated in time (2). Durand (1) suggested that subtle differences in staining intensity should also be taken into account, because such differences could indicate fluctuations in flow that could also contribute to intermittent hypoxia. Accordingly, he has argued that fluctuant hypoxia is likely to be a common physiological feature of tumors.

Work from this laboratory directly supports Durand's theory and also reveal a mechanism for the pO_2 instabilities. We measured perivascular pO_2 in skin-fold window-chamber tumors, concomitantly with measurements of microvessel red cell flux in the same vessels (24). Red cell fluxes varied temporally by as much as several orders of magnitude, but typical variations averaged ~2-fold. Perivascular pO_2 was found to be directly proportional to red cell flux within each microvessel. Thus, this work provided the first direct evidence that temporal variations in microvessel red cell flux can alter tissue oxygenation. The cycle frequencies were also on the order of 2 to 3 events per hour (7). Green's function models of typical networks, predicted that as much as 30% of a tumor region could experience transient hypoxia as a result of 2-fold changes in microvessel red cell flux (24). This prediction was higher than the observed incidence of vascular stasis in this model and in other models in which dye mismatch has been evaluated by Durand and LePard (1) and Trotter *et al.* (2).

One has to be cautious about extrapolating data from a window-chamber model to a larger more three-dimensional tumor. However, laser Doppler flow studies of red cell flux instability performed in a number of preclinical models as well as in human tumors show typical cycle times of 2-to-5-per-hour variation magnitudes of a factor of 1.5- to 3-fold. Thus, these data are in the range that we predicted would be sufficient to cause transient hypoxia using the Green's function models (1, 3, 25–27).

Brurberg *et al.* published two articles recently (8, 9) that directly corroborate the notion that tumor oxygenation is temporally unstable with a frequency of a few cycles per hour. In their work, they used the Oxford Optronix fiber optic oxygen sensor to measure transients in pO_2 in multiple sites in two early-passage human tumor xenograft lines. Fourier analysis as well as the direct evaluation of the number of crossings across a 10-mm-Hg threshold showed remarkable consistency with our prior data on the R3230Ac mammary tumor and with the data in this article (6, 7).

The process of hypoxia reoxygenation injury generates free radicals, which may induce overexpression of defense mechanisms to protect cells from oxidative damage as well as being a potential cause of genetic instability (28–30). Cairns *et al.* (31) recently reported that exogenous manipulation of tumor oxygenation imposed by exposing animals to various levels of ambient oxygen can lead to increased frequency of single strand breaks and propensity toward metastasis *in vivo*.

Temporal instability in oxygenation may also have significant influence on angiogenesis. For example, we have recently shown that hypoxia-reoxygenation injury, such as that seen in this paper, leads to increases in the transcription of pro-angiogenic genes regulated by the hypoxia responsive promoter, hypoxia inducible factor-1 (HIF-1; Ref. 32). Two sources of increased HIF-1 activity were described. The first was related to stabilization of HIF-1α created by the presence of elevated levels of reactive oxygen species. The second mechanism involved disaggregation of hypoxia-mediated stress granules during reoxygenation. It was shown that these granules contained protected pro-angiogenic HIF-1-mediated mRNA transcripts, such as vascular endothelial growth factor and plasminogen activator inhibitor 1.

Causes of Temporal pO_2 Instability in Tumors. There are at least four potential causes of fluctuant hypoxia: arteriolar vasomotion, vascular remodeling, variations in distribution of red cells at bifurcation points, and changes in oxygen consumption rate. Intaglietta *et al.* (33) used skin-fold window-chamber tumors to examine tumor-feeding arteriolar diameter while simultaneously examining downstream microvessel red cell flux. They noted temporal coordination in these events and suggested that arteriolar vasomotion could cause transient variations in perfusion that could be important for drug and nutrient transport (33). We have performed serial measurements of tumor arteriolar diameter, while simultaneously measuring downstream microvessel red cell flux. In some instances, the two processes appear to be temporally coordinated and occur with a periodicity of 2 to 3 cycles per hour (34, 35). This result suggests that arteriolar vasomotion may contribute to the temporal instability in red cell flux and vascular oxygenation in some cases. However, coordination between these events did not always occur, and this suggests that there are likely other mechanisms playing a role.

Vascular remodeling that occurs during tumor angiogenesis may be another key factor. Patan *et al.* (36), used skin-fold window chambers to perform serial observations of vascular architecture over periods of 1 to 2 hours. They commonly observed evidence for vascular intussusception, a process of vascular remodeling that would cause changes in microvessel flow resistance. The process of intussusception involves the in-growth of endothelial pillars into a vascular lumen, the consequence of which is to split a vessel segment into two or more smaller diameter vessels.

Variations in how red cells distribute at bifurcations can also alter flow resistance because microvessel hematocrit directly influences flow resistance (37). The influence of variations in red cell distribution on flow resistance would be exaggerated in tumors because the microenvironmental conditions cause reduced red cell membrane fluidity and an increased propensity toward Rouleaux formation (38).

Fourier Analysis of Changes in Frequency and Power in pO_2 and Blood Flow after Switch from Air to O_2 Breathing. Fourier analysis showed significant changes in power and frequency of pO_2 fluctuations when switching from air to O_2 breathing for both types of tumors. Analysis of FSA traces showed an increase in frequency and power of fluctuations after O_2 breathing began. Conversely, hyperoxic breathing had a dampening effect on the power of the 9L pO_2, significantly decreasing the magnitude but not the frequency of the pO_2 fluctuations.

The frequency and magnitude of blood flow fluctuations did not change significantly for FSA or 9L tumors with the onset of O_2

breathing. However, blood flow was measured using laser Doppler probes, which measure over larger areas of tissue than do microelectrodes (sensor diameter, ~200 μm compared with 6 μm for polarographic electrodes; Ref. 14). The lack of a measured concurrent change in blood flow could be due to the difference in spatial resolution between the two methods of measurement. Changes in microregional blood flow could be occurring over spatial volumes that are not measurable with laser Doppler. Similarly, microregional changes in flow could be occurring in different directions, such that when averaged over a relatively large volume, they yield no net change in flow as detected by laser Doppler.

This is the first report showing that oxygen breathing can affect O_2 transients and that there are tumor-specific effects. The cause of these changes in frequency and magnitude of the pO_2 fluctuations in tumors during air and O_2 breathing is unknown, but one possible reason for the fluctuations in pO_2 and blood flow may be changes in red blood cell flux induced by changes in vasomotor activity of tumor arterioles. Future work will examine potential mechanisms.

Limitations of Study and Future Directions. The data reported in this study are limited to roughly a 1-hour period of observation. It is possible that fluctuations occur over longer time intervals. Vascular remodeling, as occurs concomitantly with angiogenesis, could contribute to this process. A recent study using matched hypoxia markers showed that up to 15% of tumor cells may experience transient changes in oxygenation over a 12-hour period (5).

An important unknown with respect to fluctuant hypoxia is the size of regions that are affected. Does fluctuant hypoxia occur at the individual microvessel level, or are the fluctuations coordinated over small networks or an entire tumor? Existing data suggest that fluctuant hypoxia is not at the individual microvessel level. Temporal fluctuations in microvessel red cell flux in small groups (regions with 200–500-μm diameters) of microvessels is typically coordinated (24). Vascular stasis, on the other hand, tends to occur sporadically (5–10% incidence) and involves single-vessel segments (34). The two papers by Brurberg *et al.* (8, 9) also substantiate that at least small microregions are being affected, as assessed by multiple Oxford Optronix sensors within individual tumors. These results suggest that the variations in red cell flux are not controlled at the whole tumor level. However, the probes are quite large, relative to the oxygen diffusion distance and sample a surface area around the probe tip that is 3.8×10^4 μm^2 (14). A square region this size would be ~190 μm in length. Such microregions would contain several microvessels (39). These results, then, suggest that the variations in red cell flux and consequent pO_2 occur over regions that comprise at least small groups of vessels (8, 9). Additional work is needed to clarify this issue further.

Issues Related to Data Interpretation and Methods of Analysis: Effect of Measurement Device Drift on Fluctuations in Red Cell Flux and pO_2. We have ruled out the possibility that the fluctuations in pO_2 and red cell flux are due to drift in the measurement devices. First, the most compelling evidence comes from the work of Kimura *et al.* (24). In those experiments, red cell flux of individual microvessels was measured directly in-window-chamber tumors by observing the movement of fluorescently labeled red cells. Second, the ranking of power spectra for laser Doppler flow and pO_2 showed that the measurement for the 9L tumor was greater than that for the FSA. The fact that these two methods independently ranked the 9L tumor as having greater instability is indirect evidence that the fluctuations are not due to measurement drift. Finally, when the oxygen electrodes are calibrated *in vitro*, the currents obtained at set levels of oxygen are very stable ($<$1.0 mm Hg), indicating little or no drift.

Baseline instabilities in pO_2 and laser Doppler flow cause some difficulty in interpreting the response of the tissue to any oxygen-manipulation protocol. Because it is not possible to obtain a stable baseline value, the challenge is to distinguish changes in pO_2 or blood flow that are caused by a physiological manipulation from fluctuation in these values due to the underlying physiology. In prior work, we developed a Baysian statistics method to distinguish changes in pO_2 created by a manipulation from random fluctuation (40). Although Baysian statistics were not used in this article, the results are fairly typical of what we observed in the prior Baysian analysis for the R3230Ac tumor (40).

The change in Fourier transform results, after the switch from air to oxygen breathing, is less subject to interpretation errors because the data are obtained from blocks of time before and after the manipulation. Fourier analysis of a discrete sample assumes that the sample has periodic events with constant frequencies over the period of observation. Nothing was done during the experiments that would invalidate this assumption.

ACKNOWLEDGMENTS

We thank the statistical programming support provided by Anne Maumary-Gremaud and technical support provided by Jennifer Lanzen. The 9L tumor line was obtained as a generous gift from Dr. Kenneth Wheeler. The immunohistochemistry was provided by Dr. Zahid Rabbani.

REFERENCES

1. Durand RE, LePard NE. Contribution of transient blood flow to tumour hypoxia in mice. Acta Oncol 1995;34:317–23.
2. Trotter MJ, Chaplin DJ, Durand RE, Olive PL. The use of fluorescent probes to identify regions of transient perfusion in murine tumors. Int J Radiat Oncol Biol Phys 1989;16:931–4.
3. Chaplin DJ, Hill SA. Temporal heterogeneity in microregional erythrocyte flux in experimental solid tumours. Br J Cancer 1995;71:1210–3.
4. Rijken PF, Bernsen HJ, Peters JP, Hodgkiss RJ, Raleigh JA, van der Kogel AJ. Spatial relationship between hypoxia and the (perfused) vascular network in a human glioma xenograft: a quantitative multi-parameter analysis. Int J Radiat Oncol Biol Phys 2000;48:571–82.
5. Bennewith KL, Raleigh JA, Durand RE. Orally administered pimonidazole to label hypoxic tumor cells. Cancer Res 2002;62:6827–30.
6. Dewhirst MW, Braun RD, Lanzen JL. Temporal changes in PO2 of R3230AC tumors in Fischer-344 rats. Int J Radiat Oncol Biol Phys 1998;42:723–6.
7. Braun RD, Lanzen JL, Dewhirst MW. Fourier analysis of fluctuations of oxygen tension and blood flow in R3230Ac tumors and muscle in rats. Am J Physiol 1999;277:H551–68.
8. Brurberg KG, Graff BA, Olsen DR, Rofstad EK. Tumor-line specific pO(2) fluctuations in human melanoma xenografts. Int J Radiat Oncol Biol Phys 2004;58:403–9.
9. Brurberg KG, Graff BA, Rofstad EK. Temporal heterogeneity in oxygen tension in human melanoma xenografts. Br J Cancer 2003;89:350–6.
10. Grant JP, Wells SA Jr. Tumor resistance in rats immunized to fetal tissues. J Surg Res 1974;16:533–40.
11. Wheeler KT, Tel N, Williams ME, Sheppard S, Levin VA, Kabra PM. Factors influencing the survival of rat brain tumor cells after in vitro treatment with 1,3-bis(2-chloroethyl)-1-nitrosourea. Cancer Res 1975;35:1464–9.
12. Linsenmeier RA, Yancey CM. Improved fabrication of double-barreled recessed cathode O2 microelectrodes. J Appl Physiol 1987;63:2554–7.
13. Schneiderman G, Goldstick TK. Oxygen electrode design criteria and performance characteristics: recessed cathode. J Appl Physiol 1978;45:145–54.
14. Braun RD, Lanzen JL, Snyder SA, Dewhirst MW. Comparison of tumor and normal tissue oxygen tension measurements using OxyLite or microelectrodes in rodents. Am J Physiol Heart Circ Physiol 2001;280:H2533–44.
15. Raleigh JA, Chou SC, Tables L, Suchindran S, Varia MA, Horsman MR. Relationship of hypoxia to metallothionein expression in murine tumors. Int J Radiat Oncol Biol Phys 1998;42:727–30.
16. Buerk DG, Riva CE. Vasomotion and spontaneous low-frequency oscillations in blood flow and nitric oxide in cat optic nerve head. Microvasc Res 1998;55:103–12.
17. Braun RD, Linsenmeier RA, Yancey CM. Spontaneous fluctuations in oxygen tension in the cat retina. Microvasc Res 1992;44:73–84.
18. Smith TL, Osborne SW, Hutchins PM. Long-term micro- and macrocirculatory measurements in conscious rats. Microvasc Res 1985;29:360–70.
19. Jenkins WT, Evans SM, Koch CJ. Hypoxia and necrosis in rat 9L glioma and Morris 7777 hepatoma tumors: comparative measurements using EF5 binding and the Eppendorf needle electrode. Int J Radiat Oncol Biol Phys 2000;46:1005–17.
20. Kavanagh MC, Tsang V, Chow S, et al. A comparison in individual murine tumors of techniques for measuring oxygen levels. Int J Radiat Oncol Biol Phys 1999;44:1137–46.
21. Fenton BM, Kiani MF, Siemann DW. Should direct measurements of tumor oxygenation relate to the radiobiological hypoxic fraction of a tumor? Int J Radiat Oncol Biol Phys 1995;33:365–73.

22. Kirkpatrick JP, Cardenas-Navia LI, Dewhirst MW. Predicting the effect of temporal variations in pO(2) on tumor radiosensitivity. Int J Radiat Oncol Biol Phys 2004;59: 822–33.
23. Wouters BG, Brown JM. Cells at intermediate oxygen levels can be more important than the "hypoxic fraction" in determining tumor response to fractionated radiotherapy. Radiat Res 1997;147:541–50.
24. Kimura H, Braun RD, Ong ET, et al. Fluctuations in red cell flux in tumor microvessels can lead to transient hypoxia and reoxygenation in tumor parenchyma. Cancer Res 1996;56:5522–8.
25. Tufto I, Rofstad EK. Transient perfusion in human melanoma xenografts. Br J Cancer 1995;71:789–93.
26. Rofstad EK, Maseide K. Radiobiological and immunohistochemical assessment of hypoxia in human melanoma xenografts: acute and chronic hypoxia in individual tumours. Int J Radiat Biol 1999;75:1377–93.
27. Pigott KH, Hill SA, Chaplin DJ, Saunders MI. Microregional fluctuations in perfusion within human tumours detected using laser Doppler flowmetry. Radiother Oncol 1996;40:45–50.
28. Royds JA, Dower SK, Qwarnstrom EE, Lewis CE. Response of tumour cells to hypoxia: role of p53 and NFkB. Mol Pathol 1998;51:55–61.
29. Reynolds TY, Rockwell S, Glazer PM. Genetic instability induced by the tumor microenvironment. Cancer Res 1996;56:5754–7.
30. Li Q, Sanlioglu S, Li S, Ritchie T, Oberley L, Engelhardt JF. GPx-1 gene delivery modulates NFkappaB activation following diverse environmental injuries through a specific subunit of the IKK complex. Antioxid Redox Signal 2001;3:415–32.
31. Cairns RA, Kalliomaki T, Hill RP. Acute (cyclic) hypoxia enhances spontaneous metastasis of KHT murine tumors. Cancer Res 2001;61:8903–8.
32. Moeller BJ, Cao Y, Vujaskovic Z, Dewhirst MW. Reactive oxygen species and hypoxia inducible factor-1alpha serve as important vascular stabilizing elements in tumors following radiotherapy. Int J Radiat Oncol Biol Phys 2003;57(Suppl): S320–1.
33. Intaglietta M, Myers RR, Gross JF, Reinhold HS. Dynamics of microvascular flow in implanted mouse mammary tumours. Bibl Anat 1977;15:273–6.
34. Dewhirst MW, Kimura H, Rehmus SW, et al. Microvascular studies on the origins of perfusion-limited hypoxia. Br J Cancer Suppl 1996;27:S247–51.
35. Dewhirst MW, Ong ET, Rosner GL, et al. Arteriolar oxygenation in tumour and subcutaneous arterioles: effects of inspired air oxygen content. Br J Cancer Suppl 1996;27:S241–6.
36. Patan S, Munn LL, Jain RK. Intussusceptive microvascular growth in a human colon adenocarcinoma xenograft: a novel mechanism of tumor angiogenesis. Microvasc Res 1996;51:260–72.
37. Kiani MF, Pries AR, Hsu LL, Sarelius IH, Cokelet GR. Fluctuations in microvascular blood flow parameters caused by hemodynamic mechanisms. Am J Physiol 1994; 266:H1822–8.
38. Kavanagh BD, Coffey BE, Needham D, Hochmuth RM, Dewhirst MW. The effect of flunarizine on erythrocyte suspension viscosity under conditions of extreme hypoxia, low pH, and lactate treatment. Br J Cancer 1993;67:734–41.
39. Secomb TW, Hsu R, Braun RD, Ross JR, Gross JF, Dewhirst MW. Theoretical simulation of oxygen transport to tumors by three-dimensional networks of microvessels. Adv Exp Med Biol 1998;454:629–34.
40. Muller P, Rosner G, LYT I, Dewhirst MWA. Bayesian model for detecting acute change in nonlinear profiles. J Am Stat Assoc 2001;96:1215–22.